

20. Q. Ouyang, J.-M. Flesseles, *Nature* **379**, 143 (1996).
21. D. Battogtokh, A. S. Mikhailov, *Physica D* **90**, 84 (1996).
22. D. Battogtokh, A. Preusser, A. S. Mikhailov, *Physica D* **106**, 327 (1997).
23. H. H. Rotermund, W. Engel, M. Kordesch, G. Ertl, *Nature* **343**, 355 (1990).
24. H. H. Rotermund, *Surf. Sci. Rep.* **29**, 265 (1997).
25. The apparatus is equipped with low-energy electron diffraction, Auger electron spectroscopy, differentially pumped quadrupole mass spectroscopy, Ar-ion sputtering, and resistive sample heating. Using microlithography methods, we deposited a thin Ti layer surrounding areas of clean Pt. In situ oxidation of the Ti layer in the UHV chamber produces a TiO<sub>2</sub> layer. Because TiO<sub>2</sub> is not catalytically active for the CO oxidation, isolated surface reactors could thus be created. Such isolated prefabricated reactors of various sizes occupy ~80% of the entire sample surface. For the experiment, a 1-mm<sup>2</sup> reactive region is chosen. The sample is prepared by repeated cycles of Ne sputtering and O<sub>2</sub> treatment at 470 K and subsequent annealing to 750 K.
26. The instrument's field-of-view is chosen at 500 μm in diameter, and the spatial resolution of images is typically 1 μm. The PEEM images are recorded by a video camera at a rate of 40 ms per frame.
27. The PEEM intensity is defined so that the darker image areas have a higher intensity.
28. M. Kim *et al.*, unpublished data.
29. K. Krischer, M. Eiswirth, G. Ertl, *J. Chem. Phys.* **96**, 9161 (1992).
30. A. von Oertzen, A. S. Mikhailov, H. H. Rotermund, G. Ertl, *J. Phys. Chem. B* **102**, 4966 (1998).
31. Y. Pomeau, *Physica D* **23**, 3 (1986).
32. M. Argentina, P. Coulet, *Phys. Rev. E* **56**, R2359 (1997).
33. We gratefully acknowledge Y. Kevrekidis for help with microlithographic fabrication of the crystal samples used in these experiments.

1 February 2001; accepted 9 April 2001

# Bacterial Recognition of Mineral Surfaces: Nanoscale Interactions Between *Shewanella* and α-FeOOH

Steven K. Lower,<sup>1\*</sup> Michael F. Hochella Jr.,<sup>1</sup> Terry J. Beveridge<sup>2</sup>

Force microscopy has been used to quantitatively measure the infinitesimal forces that characterize interactions between *Shewanella oneidensis* (a dissimilatory metal-reducing bacterium) and goethite (α-FeOOH), both commonly found in Earth near-surface environments. Force measurements with subnanometer resolution were made in real time with living cells under aerobic and anaerobic solutions as a function of the distance, in nanometers, between a cell and the mineral surface. Energy values [in attojoules (10<sup>-18</sup> joules)] derived from these measurements show that the affinity between *S. oneidensis* and goethite rapidly increases by two to five times under anaerobic conditions in which electron transfer from bacterium to mineral is expected. Specific signatures in the force curves suggest that a 150-kilodalton putative iron reductase is mobilized within the outer membrane of *S. oneidensis* and specifically interacts with the goethite surface to facilitate the electron transfer process.

The Fe(II)-Fe(III) redox cycle represents a major energy flux at Earth's surface. A critical component of this system is the reduction of iron-containing minerals by biological processes (1, 2). *Shewanella*—a Gram-negative, dissimilatory metal-reducing bacterium found in soils, sediments, surface waters, and ground waters—is able to conserve energy for growth by using oxygen or ferric iron as a terminal electron acceptor (3, 4). In many natural environments, oxygen is in limited supply, but Fe(III) is present as a major element in the crystal structure of minerals. Hence, dissimilatory metal-reducing bacteria often oxidize various carbon substrates by reductively dissolving Fe(III)-containing minerals, the most ubiquitous in the near-

surface environments being iron oxyhydroxides (such as ferrihydrite, goethite, and hematite) (5–12). This affects a wide array of processes, including the biogeochemical cycle of iron and phosphorus, the oxidation of natural and anthropogenic carbon sources, biocorrosion, and the release of heavy metals associated with iron oxyhydroxides.

The dissimilatory reduction of iron-containing minerals presents a rather unique situation because, unlike oxygen, Fe(III) in a solid form cannot diffuse across the cell wall to the plasma membrane which, in most bacteria, houses the proteins involved in electron transfer, proton translocation, and the subsequent generation of adenosine triphosphate. Microorganisms like *Shewanella* may be able to generate two energized membranes using a unique system of proteins that shuttle electrons from an energy source in the cytoplasm, across the plasma membrane and periplasmic space, to the outer membrane (13, 14). Once in the outer membrane, iron reductases appear to transfer electrons directly to Fe(III) in the crystal structure of minerals, causing a weakening of the iron-oxygen bond and reductive dissolution of the mineral (6, 15–18). A great deal of research has

focused independently on either the microbiological or mineralogical aspects of the interaction between *Shewanella* and iron oxyhydroxides. However, few studies have been conducted on the interface between the bacterium and iron-containing minerals. It is this interface, delineated by chemical and structural features on the surface of the organism (such as concentration and localization of cytochromes and reductases and the physical structure of the outer membrane) and the mineral surface (such as density and coordination of iron-oxide moieties, surface microtopography, and crystallographic orientation), which probably has a major impact on the kinetics and extent of bacterial reduction of Fe(III) minerals.

We used biological force microscopy (19, 20) to probe the interface between a living cell of *Shewanella oneidensis*, formerly classified as *S. putrefaciens* MR-1 (21), and the (010) surfaces of goethite (α-FeOOH) and diaspore (α-AlOOH, which is isostructural with goethite and has surface properties such as charge and hydrophobicity that are similar to those of goethite) at the nanoscale level in anaerobic and aerobic solutions. *S. oneidensis* was grown under anaerobic conditions using lactate as the carbon and energy source and Fe(III)-citrate as the electron acceptor (22). To preserve the natural, complex biomolecular network on the surface of the bacteria, fully functional cells (measuring 0.5 by 2 μm) were linked in their native state to a small bead (radius 5 μm) situated on the end of a silicon nitride cantilever thereby creating a biologically active force probe (23). A commercial force microscope (NanoScope IIIa Multimode scanning probe microscope, Digital Instruments, Santa Barbara, CA) was used to measure the deflection of a biologically active force probe by reflecting a laser off the top of the cantilever and into a photodiode detector while an oriented mineral crystal, mounted on a piezoelectric scanner, was translated toward (generating approach data), made contact with, and was subsequently retracted from (generating retraction data) a bacterium on the probe (24). Photodiode response (in volts) was converted to cantilever deflection (in meters) using a conversion factor (in meters per volt) determined from the photodiode shift voltage (25). Cantilever deflection was multiplied by the cantilever spring constant [ $k_{sp} = 0.07 \text{ N m}^{-1}$ , determined

<sup>1</sup>NanoGeoscience and Technology Laboratory, Department of Geological Sciences, Virginia Polytechnic Institute and State University, Blacksburg, VA 24061, USA. <sup>2</sup>Department of Microbiology, College of Biological Science, University of Guelph, Guelph, Ontario N1G 2W1, Canada.

\*To whom correspondence should be addressed. E-mail: slower@vt.edu Present address: Department of Geology, University of Maryland, College Park, MD 20742, USA.

## REPORTS

as described previously (26)], to calculate the force of interaction (in newtons). Displacement of the mineral on the piezoelectric scanner was converted to separation (or distance) between

the bacterium and the mineral by correcting for cantilever deflection (27) and selecting the point of contact using jump-to-contact and jump-from-contact events for approach and retraction

curves, respectively. For retraction curves, it is more appropriate to refer to extension rather than the distance between a bacterium and the mineral because polymers on a cell surface form a bridge with the mineral.

In a typical experiment with goethite, approach and retraction forces were measured after varying the contact time between *S. oneidensis* and the mineral in anaerobic solutions supplemented with lactate as an energy source (Fig. 1A). An aerobic solution supplemented with lactate was then injected into the fluid cell of the force microscope and allowed to incubate for 30 min, after which forces were again measured as a function of the contact time between the bacterium and the mineral (Fig. 1B). Rather than comparing individual force datum points (such as the maximum force of adhesion), as is typically done with force microscopy, we determined energy values by integrating force with respect to distance (Table 1). This use of entire data sets allowed a more thorough characterization of the complex physical and chemical intricacies involved in these reactions. In general, the retraction curves may help explain the transfer of electrons from biomolecules on *S. oneidensis* to iron atoms in goethite, because direct cell-to-mineral contact is generally, although not always (28), considered a prerequisite for this reaction (6, 17, 29, 30). The approach curves, on the other hand, give an estimate of the intermolecular forces that will effect whether *S. oneidensis* is able to bridge the solution gap between itself and the mineral.

For the approach curves, repulsion between *S. oneidensis* and goethite under anaerobic conditions was greater after the bacterium and the mineral remained in contact for 30 to 45 min (Fig. 1A and Table 1). Infusion of an oxygenated solution caused the bacterium to alter its surface so that this repulsive interaction decreased to the point where it became slightly attractive (Fig. 1B and Table 1). The point of zero charge (or isoelectric point) of *Shewanella* is 5 to 6 (determined under aerobic conditions) (31) and 7 to 8 for goethite (32). On the basis of electrostatic considerations, a slight attraction would be expected at a pH of ~6. However, there is a high degree of electrochemical heterogeneity on the surface of *Shewanella*, and its surface charge is dependent on the concentration and localization of at least five different types of functional groups that are arrayed over the cell surface (31). Under aerobic conditions, amine-groups are embedded within the outer membrane and underlying peptidoglycan layer so that they do not contribute to the surface charge (31). Anaerobic conditions induce the expression of proteins in the outer membrane of *S. oneidensis* (15–17). The amine groups on these proteins may lead to an increased positive charge on the cell surface so that repulsion would be expected between *S. oneidensis* and goethite in anaerobic solutions, as observed in approach curves (Fig. 1A).

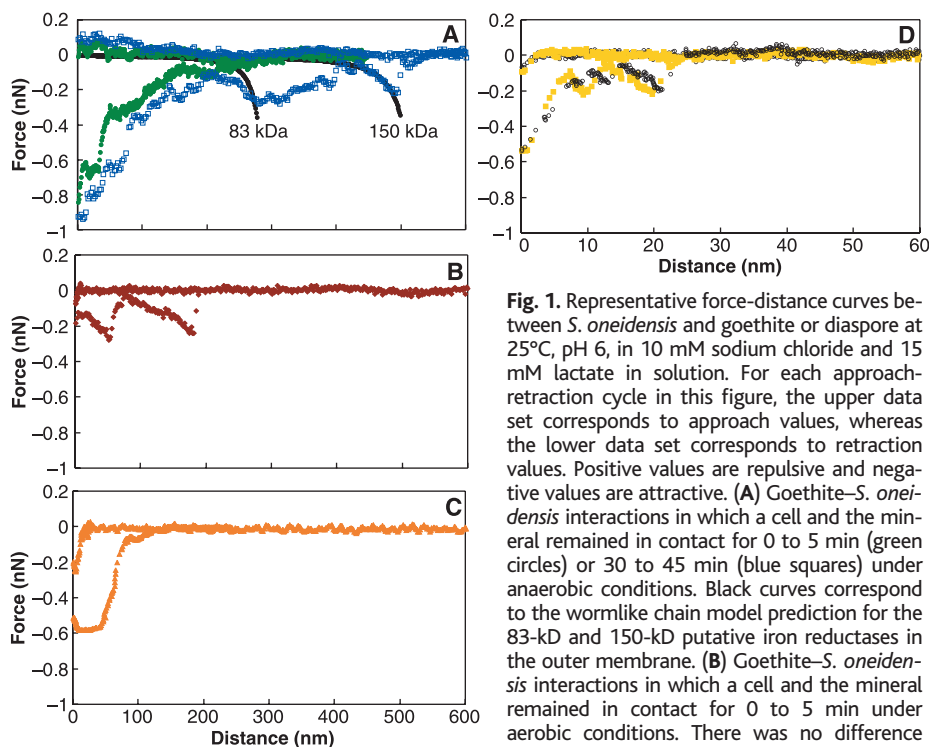


**Fig. 1.** Representative force-distance curves between *S. oneidensis* and goethite or diaspore at 25°C, pH 6, in 10 mM sodium chloride and 15 mM lactate in solution. For each approach-retraction cycle in this figure, the upper data set corresponds to approach values, whereas the lower data set corresponds to retraction values. Positive values are repulsive and negative values are attractive. (A) Goethite-*S. oneidensis* interactions in which a cell and the mineral remained in contact for 0 to 5 min (green circles) or 30 to 45 min (blue squares) under anaerobic conditions. Black curves correspond to the wormlike chain model prediction for the 83-kD and 150-kD putative iron reductases in the outer membrane. (B) Goethite-*S. oneidensis* interactions in which a cell and the mineral remained in contact for 0 to 5 min under aerobic conditions. There was no difference between the 0-to-5-min and 30-to-45-min

contact under aerobic conditions (see Table 1 for comparison). (C) Diaspore-*S. oneidensis* interactions under aerobic conditions. There was no difference between the aerobic and anaerobic experiments between diaspore and *S. oneidensis* (see Table 1 for comparison). (D) Interactions between goethite and a nonviable cell of *S. oneidensis* under anaerobic (gold squares) or aerobic (black circles) conditions. Note the difference in the scale of the distance axis.

**Table 1.** Force and energy measurements for the interactions between *S. oneidensis* and goethite or diaspore in anaerobic or aerobic solutions. Results are reported as a function of the amount of contact time between the bacteria and the mineral before biological force microscopy measurements. Force values [in picoNewtons ( $10^{-12}$  N)] are the maximum magnitude recorded in approach or retraction curves and as such represent only one datum point for each. Energy values [in attojoules ( $10^{-18}$  J)] are calculated by integrating force with respect to distance and as such incorporate the entire data set. These values represent the average  $\pm$  SD results of over 500 force measurements conducted with four *S. oneidensis* biologically active force probes. Positive numbers are repulsive; negative numbers are attractive.

Mineral	Approach		Retraction	
	Force (pN)	Energy (aj)	Force (pN)	Energy (aj)
<i>Anaerobic</i>				
Goethite (0–5 min)	59 $\pm$ 36	3.5 $\pm$ 1.9	–747 $\pm$ 115	–59.5 $\pm$ 8.7
Goethite (30 to 45 min)	104 $\pm$ 49	6.7 $\pm$ 2.5	–795 $\pm$ 145	–136.7 $\pm$ 20.7
Diaspore (30 to 45 min)	–237 $\pm$ 68	–3.2 $\pm$ 2.8	–397 $\pm$ 164	–39.2 $\pm$ 7.4
<i>Aerobic</i>				
Goethite (0 to 5 min)	–54 $\pm$ 22	–0.5 $\pm$ 0.4	–248 $\pm$ 109	–26.2 $\pm$ 6.1
Goethite (30 to 45 min)	–35 $\pm$ 14	–1.0 $\pm$ 0.4	–253 $\pm$ 95	–27.1 $\pm$ 9.6
Diaspore (30 to 45 min)	–271 $\pm$ 61	–3.1 $\pm$ 1.3	–433 $\pm$ 127	–41.2 $\pm$ 4.2

## REPORTS

Retraction curves represent in many cases a complex dynamic of adhesion involving, among other things, bond breaking, intermolecular forces, and extension of outer membrane biomolecules that form a bridge between a bacterium and the mineral surface. Under aerobic conditions, *S. oneidensis* exhibited a stronger overall energy of adhesion to diaspore relative to goethite (Fig. 1, B and C, and Table 1). Under anaerobic conditions, *S. oneidensis* exhibited an increased affinity for goethite, as indicated by the retraction curves and energy calculations (Fig. 1A and Table 1), whereas the attractive energy between diaspore and *S. oneidensis* was indifferent to oxygen concentrations in the solutions (Table 1). The retraction energies between *S. oneidensis* and goethite were 2 to 5 times stronger under anaerobic as opposed to aerobic conditions (Table 1). Under anaerobic conditions, this attraction increased with the amount of contact time for goethite (Table 1) but not for diaspore. Biologically active force probes fabricated with nonviable cells exhibited an attraction toward goethite, but this affinity did not change with oxygen concentration in the solution (Fig. 1D). Taken together, this indicates that the adhesion between *S. oneidensis* and goethite is due, at least in part, to processes associated with dissimilatory iron reduction, and provides direct evidence suggesting that the bacteria actively recognize the goethite surface so that they localize and/or produce biomolecules at the mineral interface. This type of recognition between a microorganism and a mineral surface has been suggested but never quantified (33, 34). This could be one of the functions of the fluidity of the outer membrane, allowing the bacterium to react rapidly to the mineral surface and to congregate reactive membrane macromolecules at sites of contact. Dynamic modeling of outer membrane lipopolysaccharides suggests molecular motion over microsecond time frames (35), and it is possible that cytochromes and reductases could also have rapid motional attributes.

Anaerobic retraction curves between goethite and *S. oneidensis* exhibit a strong force of interaction within the first few hundred nanometers, followed by a jagged plateau (Fig. 1A). In many cases, the retraction curves terminate in this sawtoothlike discontinuity (Fig. 1A), which we suggest is a signature of the unfolding of outer membrane proteins that form a bridge between a living bacterium and the mineral surface (36). The sawtoothlike patterns in the retraction curves were analyzed to gain more definitive evidence for the presence of outer membrane proteins that may be involved in the direct transfer of electrons from the cell to the min-

eral. A total of four putative iron-reductases ranging in size from 53 to 150 kD have been isolated from the outer membrane of *S. oneidensis* (17, 18). According to the wormlike chain model (37), which can be used to calculate the force ( $F$ ) needed to stretch a polypeptide chain in a solvent to a length  $x$ ,  $F(x) = (kT/b) [0.25(1 - x/L)^{-2} - 0.25 + x/L]$ , where  $k$  is the Boltzmann's constant;  $T$  is the temperature;  $b$  is the persistence length (that is, the length of the stiff segment of the chain), which is 0.38 nm for the distance between two  $C_{\alpha}$  atoms in a polypeptide (38–40); and  $L$  is the contour length (that is, the length of the completely stretched chain) calculated for each putative iron reductase, assuming an average molecular mass of 110 daltons per amino acid residue (18, 41) and an average molecular length of 0.4 nm per amino acid residue (39).

Of the four putative iron reductases, the 83-kD protein has been the only one to be fully characterized in previous reports (17, 18); however, recent studies involving mutants incapable of producing this protein provide evidence that it is not an iron reductase (42). Predictions based on the wormlike chain model, when compared to our anaerobic retraction curves (Fig. 1A), are consistent with this. Of the remaining three putative iron reductases, the wormlike chain model prediction for the 150-kD protein fit 82% of the retraction curves for *S. oneidensis* and goethite under anaerobic conditions and longer contact times (Fig. 1A). Evidence of this protein was not found in the retraction curves of the aerobic-goethite system (Fig. 1B), the diaspore experiments (Fig. 1C), or the experiments with nonviable cells (Fig. 1D). This strongly suggests that the 150-kD protein in the outer membrane of *S. oneidensis* specifically interacts with the surface of goethite, fulfilling some aspect of the electron transfer reaction (43).

We have shown that under anaerobic conditions, *S. oneidensis* responds to the surface of goethite by rapidly developing stronger adhesion energies at the interface. We interpret these data to indicate that after recognition of goethite as a terminal electron acceptor, *S. oneidensis* actively mobilizes and/or produces proteins (the 150-kD putative reductase and perhaps others) that specifically interact with the mineral surface. This is an example of using nanomechanical measurements and properties to help isolate likely biochemical and mineralogical mechanisms that operate under environmentally relevant conditions. In addition, besides an improved fundamental understanding of bacterial interactions with solid surfaces, the ability to quantitatively probe and characterize these specific interactions in dimensional, force, and energy nanospace could lead to advances in nanotechnology. For example, one may now be able to systematically tailor the exquisite natural specificity between biomolecules, as produced by living microorganisms, and material surfac-

es for the purposes of chemical and/or structural nanoscale modification of the cell, the material surface, or both.

### References and Notes

1. D. R. Lovley, *Microbiol. Rev.* **55**, 259 (1991).
2. K. H. Nealson, D. Saffarini, *Annu. Rev. Microbiol.* **48**, 311 (1994).
3. R. G. Arnold, M. R. Hoffmann, T. J. DiChristina, F. W. Picardal, *Appl. Environ. Microbiol.* **56**, 2811 (1990).
4. C. R. Myers, K. H. Nealson, *J. Bacteriol.* **172**, 6232 (1990).
5. D. R. Lovley, E. J. P. Phillips, *Appl. Environ. Microbiol.* **52**, 751 (1986).
6. R. G. Arnold, T. J. DiChristina, M. R. Hoffmann, *Bio-tech. Bioeng.* **32**, 1081 (1988).
7. D. R. Lovley, E. J. P. Phillips, *Appl. Environ. Microbiol.* **54**, 1472 (1988).
8. E. E. Roden, J. M. Zachara, *Environ. Sci. Tech.* **30**, 1618 (1996).
9. F. Caccavo Jr., P. C. Schamberger, K. Keiding, P. H. Nielsen, *Appl. Environ. Microbiol.* **62**, 3837 (1997).
10. J. K. Fredrickson et al., *Geochim. Cosmochim. Acta* **62**, 3239 (1998).
11. J. M. Zachara et al., *Am. Mineral.* **83**, 1426 (1998).
12. M. M. Urrutia, E. E. Roden, J. M. Zachara, *Environ. Sci. Tech.* **33**, 4022 (1999).
13. C. R. Myers, J. M. Myers, *J. Bacteriol.* **179**, 1143 (1997).
14. J. M. Myers, C. R. Myers, *J. Bacteriol.* **182**, 67 (2000).
15. C. R. Myers, J. M. Myers, *J. Bacteriol.* **174**, 3429 (1992).
16. ———, *FEMS Microbiol. Lett.* **108**, 15 (1993).
17. ———, *Biochim. Biophys. Acta* **1326**, 307 (1997).
18. J. M. Myers, C. R. Myers, *Biochim. Biophys. Acta* **1373**, 237 (1998).
19. S. K. Lower, C. J. Tadanier, M. F. Hochella Jr., *Geochim. Cosmochim. Acta* **64**, 3133 (2000).
20. S. K. Lower, C. J. Tadanier, M. F. Hochella Jr., *Geomicrobiol. J.* **18**, 63 (2001).
21. K. Venkateswaran et al., *Int. J. Sys. Bacteriol.* **49**, 705 (1999).
22. *S. oneidensis* (American Type Culture Collection no. 700550) was transformed with plasmid pSMC2, which codes for a constitutive, intracellular, green fluorescent protein (44). Transformed cells were grown in an anaerobic chamber (Coy Laboratory Products, Ann Arbor, MI) to midlogarithmic phase at room temperature as previously described (4) in a defined medium supplemented with 15 mM lactate and 2 mM ferric citrate (4).
23. Glass beads (Polysciences, Warrington, PA) were cleaned with hydrogen peroxide (30% solution), rinsed with ultrapure water, and functionalized with amino groups by incubation in a solution of 3-aminopropyltriethoxysilane (5 to 10% in acetone) for 6 hours. Previous studies have shown that linker molecules such as amino-silane have no effect on the measured bacterium-mineral interactions (19, 20). Cultured cells were rinsed three times in an anaerobic solution of 10 mM sodium chloride and were linked to functionalized glass beads by spinning the cell-bead mixture at 7000g for 2 min. A single bacteria-coated bead was then attached to a cantilever with epoxy (19). Scanning laser confocal microscopy was used to verify bacterial coverage of the probe by imaging the green fluorescent signal emitted from cells (19, 20). The viability of cells was assessed by inoculating an agar plate with a biologically active force probe after the force measurements.
24. It is difficult to quantify the area of contact between a force probe and a sample surface. Three-dimensional confocal microscopy measurements of biologically active force probes, as described previously (19, 20), suggest that a single bacterium made contact with the mineral during force measurements.
25. The region of constant compliance was not used to determine deflection, because it would have resulted in an overestimate of the measured forces because of the fact that the cells were more compliant than the cantilever (20, 45).

26. J. P. Cleveland, S. Manne, D. Bocek, P. K. Hansma, *Rev. Sci. Instrum.* **64**, 403 (1993).
27. W. A. Ducker, T. J. Senden, R. M. Pashley, *Langmuir* **8**, 1831 (1992).
28. D. K. Newman, R. Kolter, *Nature* **405**, 94 (2000).
29. T. J. DiChristina, E. F. Delong, *J. Bacteriol.* **176**, 1468 (1994).
30. A. S. Beliaev, D. A. Saffarini, *J. Bacteriol.* **180**, 6292 (1998).
31. I. Sokolov, D. S. Smith, G. S. Henderson, Y. A. Gorby, F. G. Ferris, *Environ. Sci. Tech.* **35**, 341 (2001).
32. W. Stumm, J. J. Morgan, *Aquatic Chemistry: Chemical Equilibria and Rates in Natural Waters* (Wiley, New York, ed. 3, 1996), pp 534–540.
33. S. Brown, *Proc. Natl. Acad. Sci. U.S.A.* **89**, 8651 (1992).
34. N. Ohmura, K. Kitamura, H. Saiki, *Appl. Environ. Microbiol.* **59**, 4044 (1993).
35. T. J. Beveridge, *J. Bacteriol.* **181**, 4725 (1999).
36. On the basis of transmission electron microscopy and freeze-substitution analyses, extracellular polysaccharide, a common macromolecule on the surface of many bacteria, has not been detected on the cell wall of *S. oneidensis* (A. Korenevsky and T. Beveridge, unpublished data).
37. P. J. Flory, *Statistical Mechanics of Chain Molecules* (Hanser, New York, 1989), pp. 401–403.
38. M. Rief, M. Gautel, F. Oesterhelt, J. M. Fernandez, H. E. Gaub, *Science* **276**, 1109 (1997).
39. H. Mueller, H.-J. Butt, E. Bamberg, *Biophys. J.* **76**, 1072 (1999).
40. D. J. Muller, W. Baumeister, A. Engel, *Proc. Natl. Acad. Sci. U.S.A.* **96**, 13170 (1999).
41. J.-J. Karlsson, A. Kadziola, A. Rasmussen, T. E. Rostrup, J. Ulstrup, in *Protein Folds: A Distance-Based Approach*, H. Bohr, S. Brunak, Eds. (CRC Press, Boca Raton, FL, 1996), pp. 56–67.
42. J. M. Myers, C. R. Myers, *Appl. Environ. Microbiol.* **67**, 260 (2001).
43. Future studies will use biological force microscopy with mutants incapable of producing and/or secreting cell wall biomolecules such as the 150-kD protein.
44. G. V. Bloemberg, G. A. O'Toole, B. J. J. Lugtenberg, R. Kolter, *Appl. Environ. Microbiol.* **63**, 4543 (1997).
45. N. P. D'Costa, J. H. Hoh, *Rev. Sci. Instrum.* **66**, 5096 (1995).
46. We thank B. Lower, C. Myers, J. Banfield, and the anonymous reviewers for constructive comments; G. O'Toole for providing plasmid pSMC2; and J. Tak for support. This manuscript is dedicated to B. Diehl. Mineral samples were provided by the Virginia Tech Geological Sciences Museum. Financial support was provided by the U.S. Department of Energy and the NSF.

5 February 2001; accepted 4 April 2001

# Ultrafast Source-to-Surface Movement of Melt at Island Arcs from $^{226}\text{Ra}$ - $^{230}\text{Th}$ Systematics

Simon Turner,<sup>1,2\*</sup> Peter Evans,<sup>1,3</sup> Chris Hawkesworth<sup>1,2</sup>

Island arc lavas have radium-226 excesses that extend to higher values than those observed in mid-ocean ridge or ocean island basalts. The initial ratio of radium-226 to thorium-230 is largest in the most primitive lavas, which also have the highest barium/thorium ratios, and decreases with increasing magmatic differentiation. Therefore, the radium-226 excesses appear to have been introduced into the base of the mantle melting column by fluids released from the subducting plate. Preservation of this signal requires transport to the surface arguably in only a few hundreds of years and directly constrains the average melt velocity to the order of 1000 meters per year. Thus, melt segregation and channel formation can occur rapidly in the mantle.

The velocity of melt ascent from its source through Earth's mantle and crust to the surface is extremely hard to determine, even though such measurements would place important constraints on the mechanisms of melt transport and the physical behavior of the mantle during partial melting (1–5). Disequilibria between the short-lived U-series isotopes can provide estimates of melt velocities and have recently been used to show that mantle melt velocities are too fast for transport to occur by grain-scale percolation mechanisms all the way to the surface. Instead, melt must, at some critical stage, separate into discrete channels (1–5). What remains to be determined is how quickly melt moves and at what melt fraction such channels form. The

short-lived U-series isotope  $^{226}\text{Ra}$  has a half-life of only 1600 years and can be used to estimate melt velocity and residual porosity (1–5). However, recent models for melt formation and transport beneath mid-ocean ridges and ocean islands emphasize that  $^{226}\text{Ra}$ - $^{230}\text{Th}$  disequilibria is created throughout the melting column and the disequilibria measured at the surface only reflects that produced in the upper portions of the melting column (3–5). Thus, although  $^{226}\text{Ra}$  disequilibria in mid-ocean ridge and ocean island basalts (MORB and OIB, respectively) provide important constraints on the residual porosity, they do not place tight constraints on the melt velocity because the depth of origin of the disequilibria is debatable.

No global  $^{226}\text{Ra}$  study has been conducted on island arc lavas since the pioneering investigation of Gill and Williams (6), who suggested that  $^{226}\text{Ra}$  excesses might be related to fluid addition. Accordingly, we have undertaken high-precision, mass spectrometric measurements of  $^{226}\text{Ra}$  disequilibria in 40 historic lavas from seven island arcs

that, combined with recent data from the Tonga-Kermadec arc (7), allow us to evaluate the global  $^{226}\text{Ra}$ - $^{230}\text{Th}$  systematics in island arc rocks. The  $(^{226}\text{Ra}/^{230}\text{Th})_0$  values (where the parentheses denote activity ratios) extend to  $^{226}\text{Ra}$  excesses of over 600% and show a significant variation above each arc (Table 1), ranging from 0.87 to 2.66 in the Lesser Antilles, 1.25 to 4.96 in Vanuatu, 1.51 to 1.59 in the Philippines (two samples only), 1.06 to 5.44 in the Marianas, 1.39 to 4.16 in the Aleutians, 1.00 to 3.53 in Kamchatka, 0.94 to 3.71 in Indonesia, and 0.93 to 6.13 in Tonga-Kermadec (7). Only one sample has  $(^{226}\text{Ra}/^{230}\text{Th})_0 < 1$ , and five samples are within analytical error of 1.

The  $(^{226}\text{Ra}/^{230}\text{Th})_0$  versus  $(^{238}\text{U}/^{230}\text{Th})$  diagram (Fig. 1) illustrates that the U-series disequilibria in island arc lavas are distinct from MORB and OIB, extending to higher  $(^{226}\text{Ra}/^{230}\text{Th})_0$  ratios and having the reverse sense of U-Th fractionation. Thus, the island arc lavas with the highest  $(^{226}\text{Ra}/^{230}\text{Th})_0$  are crudely correlated with the highest  $(^{238}\text{U}/^{230}\text{Th})$  (8–11). Some aspects of these different tectonic regimes are similar, in that melting is initiated at depths of 100 km and the total extent of melting is probably in the range 8 to 15%. However, for MORB and OIB, melting occurs in response to decompression. The  $^{230}\text{Th}$  excesses [i.e.,  $(^{238}\text{U}/^{230}\text{Th}) < 1$ ] reflect the greater compatibility of U, relative to Th in residual aluminous clinopyroxene and garnet (12, 13) and have been used to constrain the mantle upwelling and melting rates in these regions (1–5). The porosities required to obtain  $(^{226}\text{Ra}/^{230}\text{Th})_0 > 3$  by decompression melting alone are  $< 0.0001\%$  (1–5) and most MORB and OIB have  $(^{226}\text{Ra}/^{230}\text{Th})_0 < 3$  (Fig. 1) (14–22). In contrast, melting beneath island arcs is linked to the lowering of the peridotite solidus by addition of aqueous fluids released during dehydration reactions in the downgoing plate (23, 24), and the role of decompression on melting has proved hard to resolve (25–27). The  $^{238}\text{U}$  excesses that typify

<sup>1</sup>Department of Earth Sciences, The Open University, Walton Hall, Milton Keynes MK7 6AA, UK. <sup>2</sup>Department of Earth Sciences, Wills Memorial Building, University of Bristol, Bristol BS8 1RJ, UK. <sup>3</sup>Laboratories of the Government Geochemist, Queens Road, Teddington, Middlesex TW11 0LY, UK.

\*To whom correspondence should be addressed. E-mail: simon.turner@bristol.ac.uk